Beyond Chandra (towards the X-ray Surveyor mission): possible solutions for the implementation of very high angular resolution X-ray telescopes in the new millennium based on fused silica segments

G. Pareschi[a], S. Basso[a], M. M .Civitani[a], M. Ghigo[a], G. Parodi[b], C. Pelliciari[a], B. Salmaso[a], D. Spiga[a], G. Vecchi[a]

INAF/Brera Astronomical Observatory, Via E. Bianchi 46, 23807 Merate, Italy

ABSTRACT

An important challenge for the X-ray astronomy of the new millennium is represented by the implementation of an X-ray telescope able to maintain the exquisite angular resolution of Chandra (with a sub-arcsec HEW, on-axis) but, at the same time, being characterized by a much larger throughput and grasp. A mission with similar characteristics is represented by the X-ray Surveyor Mission. The project has been recently proposed in USA and is being currently studied by NASA. It will host an X-ray telescope with an effective area of more than 2 square meters at 1 keV (i.e. 30 times greater than Chandra) and a 15-arcminutes field-of-view, with 1-arcsecond or better half-power diameter (versus the 4 arcmin diameter of Chandra). While the scientific reasons for implementing a similar mission are clear, being related to compelling problems like e.g. the formation and subsequent growth of black hole seeds at very high redshift or the identification of the first galaxy groups and proto-clusters, the realization of a grazing-angle optics system able to fulfil these specs remain highly challenging. Different technologies are being envisaged, like e.g. the use of adjustable segmented mirrors (with use of piezoelectric or magneto-restrictive film actuators on the back surface) or the direct polishing of a variety of thin substrates or the use of innovative correction methods like e.g. differential deposition, ion-figuring or the correction of the profile via controlled stress films. In this paper we present a possible approach based on the direct polishing (with final ion figuring correction of the profile) of thin SiO_2 segmented substrates (typically 2 mm thick), discussing different aspects of the technology under implementation and presenting some preliminary results.

Keywords: X-ray mirrors, X-ray telescopes, thin fused silica segments, fine grinding, polishing, ion-beam figuring

1. INTRODUCTION

At present time there is an increasing interest by the high-energy scientific community for a mission like AXAF-Chandra [1] but with a least one order of magnitude increase in collecting area.

In this regard, it should be noted that the impressive angular resolution of Chandra (< 1 arcsec HEW) was achieved thanks to the use of thick (up to 24 mm) mirror shells together with the use of sophisticated direct polishing processes [2,3]. The Chandra optical elements have four paraboloid-hyperboloid pairs with a common 10 m focal length. The element lengths are about 0.83-m, the diameters approximately 0.63, 0.85, 0.97, and 1.2 m, and wall thickness range from 16 mm for the smaller elements to 24 mm for the outer ones. Zerodur from Schott has been the optical element material chosen because of its low coefficient of thermal expansion and demonstrated capability of permitting very smooth polished surfaces. The major fabrication phases included coarse and fine grinding, polishing, and final smoothing. The grinding and polishing operations were done with relatively small tools under computer control. Cycles were iterative; a mirror element was measured to yield an error map, appropriate tools selected to reduce the errors, and a polishing control file for the next cycle generated. The next cycle would cause more material removal in the high areas. The residual errors would be smaller than previously, and so the process converged to the required accuracies. Extending this technology to produce an X-ray telescope with one order of magnitude more of collecting area would be an impractical approach, due to the low throughput achievable with a similar wall thickness.

After the Chandra implementation, the XEUS mission has been proposed, aiming at an effective area of several m^2 and an angular resolution better than 2 arcsec HEW [4]. Unfortunately, after the initial study, this mission was not implemented, mainly due to the costs and the low level of technology readiness. The project is now evolved in the ATHENA mission [5], selected by ESA as the second "Large" mission (with a launch foreseen in 2028), aiming at the implementation of an X-ray optics based on segmented Wolter I mirrors with a maximum diameter of 3 m and an effective area of 2 m^2 [6]. For Athena the goal in terms of angular resolution is 5 arcsec HEW, to be maintained across a field-of-view of a few tens arcmin.

More recently, a proposal for such a kind of mission was the SMART-X project [7], led by CfA and involving several other US Institutes. This project then evolved in the X-ray Surveyor Mission [8]. In this regard, on January 2015 the NASA Astrophysics Division (APD) initiated a community-based process for identifying large mission candidates for prioritization by the 2020 Decadal Survey'. Among the selected missions, the X-ray Surveyor has been proposed by the US X-ray astronomy community as the future NASA large X-ray observatory that will take over Chandra. It will host an X-ray telescope with an effective area of more than 2 square meters at 1 keV (i.e. about 30 times greater than Chandra) and a 15-arcminutes field-of-view (versus the 4 arcmin diameter of Chandra) with 1 arcsecond or HEW. Now NASA has assembled a Science and Technology Definition Team (STDT) to enable a detailed Mission Concept Study, which will be used as input to the 2020 Decadal Survey (see http://wwwastro.msfc.nasa.gov/xrs/ , http://pcos.gsfc.nasa.gov/studies/xray-surveyor/).

While the scientific reasons for implementing a similar mission are clear, being related to compelling problems like e.g. the formation and subsequent growth of black hole seeds at very high redshift or the identification of the first galaxy groups and proto-clusters, the realization of a grazing-angle optics system able to fulfil these specs remain highly challenging. Different technologies are being envisaged. Among them, a branch relies on the development of specific replicated thin (typically 0.4 mm) glass segmented substrates produced via thermal slumping [9, 10, 11, 12] followed by some other correction processes in order to achieve the desired error profile requirements and angular resolution specs based on the application of controlled patterns of stress. Among these methods, one should mention the use of piezoelectric actuators [13], films with different stress levels [14] or ion implantation [15].

A different approach foresees the direct figuring and polishing of a variety of thin substrates like segments of Silicon [16], or glass and metal monolithic shells [17, 18, 19]. In this case the classical optical figuring and polishing processes may be followed by finishing methods like differential deposition [20] and ion-figuring [21]. In this paper we present a possible approach based on the direct polishing (with final ion figuring correction of the profile) of thin SiO_2 segmented substrates (typically 2 mm thick), discussing different aspects of the technology under implementation and presenting some preliminary results.

2. THE CHOICE OF FUSED SILICA FOR MAKING MIRROR SUBSTRATES SCOPE

The development of the grazing incident optics for the X-ray surveyor we are carrying out is based on the use of Fused Silica (SiO_2) substrates (with a typical thickness value is 2 mm).

Silicon dioxide occurs naturally as sand or rock and, when melted, the resulting product is called Fused Quartz. If the silicon dioxide is synthetically derived, the material is then called Fused Silica. Fused Silica (SiO_2) is therefore a synthetic molten, high purity, amorphous, non-crystalline quartz glass with exceptional properties. Typical of glasses, it lacks of a long-range order in its atomic structure. It's highly cross linked three dimensional structure gives rise to it's low thermal expansion coefficient. It is made by melting the very pure raw materials and it is used for applications, that require Fused Silica window a very good thermal strength (or whenever an excellent transparency for wavelengths below the visible spectrum is critical, but this property is not important for the fabrication of X-ray optics apart that can be useful for fastening the polymerization of glues with UV light). Due to its low coefficient of thermal expansion, quartz glass has a very good thermal shock resistance. The exceptional thermal properties enable fused silica to hold up very high thermal loads. Likewise, the high chemical stability of this unique material is one of the best. The high chemical durability of quartz glass against bases is top class and better than it is for most other glass materials. It is a material normally used in semiconductor production processes and it is also space compliant. It should be noted that the X-ray mirrors of the Einstein satellite were based on fused quartz monolithic shells [22].

Tab 1. Thermo-mechanical parameters of Fused Silica compared to other candidate materials for making the substrates of the X-ray Surveyor mirrors

PARAMETER	D263 Glass	Eagle Glass	Silicon	Fused Silica
Density (g/cm^3)	2.51	2.38	2.33	2.20
Thermal Conductivity ($W\ m^{-1}\ K^{-1}$)	0.8	1.9	148	1.37
CTE ($10^{-6}\ K^{-1}$) at 300 K	6.30	3.17	2.6	0.58
Young Modulus (GPa)	72	73.6	150	73

In Tab. 1 the main thermo-mechanical parameters of Fused Silica are reported and compared with other materials currently being considered for the realization of the X-ray Surveyor mirror walls. As it can be observed, Fused Silica is superior compared to the D263 and Eagle glasses because of a smaller density and a much lower CTE. This parameters makes Fused Silica attractive also compared to Silicon which, however, is characterized by a much larger thermal conductivity. It should be noted that Fused Silica is available in large pre-shaped substrates at an acceptable cost (very much lower of Zerodur, the glass-ceramic material used for making the Chandra's monolithic shells). It represent an excellent material to sustain optical figuring, polishing and ion-figuring thanks to its amorphous and compact micro-structure.

3. OPTO-MECHANICAL AND THERMAL PRELIMINARY CONSIDERATIONS

3.1 X-Ray Optics Design and Areal Efficiency

In order to verify if, from a mechanical and structural point of view, the realization of the mirrors for the X-ray surveyor is compliant with Fused Silica segmented shells with thickness in the 1-2 mm range, we have performed the following exercise. Six different configurations for the X-ray Surveyor's optics were considered, as summarized in Tab. 2. All designs are based on a Wolter-1-like mirror shells made of SiO_2, with a focal length of 10 m. The considered mirror length is always 0.6 m (0.3 m parabola + 0.3 m hyperbola). Designs just differ for the thickness of the mirror shells and for the external mirror diameter $ø_{MAX}$.

Tab.2 Different configurations considered for the X-ray optics of the X-Ray surveyor with mirror substrates based on SiO2 segments.

$Ø_{MAX}$	MS #	MS thick.	Envelope	A_{GROSS}	Reducing Factor	A_{GEOM}	Areal Efficiency
[m]	-	[mm]	[m^2]	[m^2]	-	[m^2]	-
3.125	170	2	7.670	5.825	0.5	2.913	0.380
3.11	183	1.5	7.596	6.086	0.5	3.043	0.401
3.125	200	1	7.670	6.528	0.5	3.264	0.426
3.62	187	2	10.292	8.06	0.5	4.030	0.392
3.61	201	1.5	10.235	8.437	0.5	4.219	0.412
3.61	218	1	10.235	8.888	0.5	4.444	0.434

$ø_{MAX}$ = Maximum (outer) diameter

MS# = Number of Mirror Shells (filling the space from a radius of 0.25 m to the outermost radius)

MS thick = Mirror Shell thickness

Envelope = Gross area corresponding to $ø_{MAX}$ (i.e. $\frac{\pi \times \Phi_{MAX}^2}{4}$)

A_{GROSS} = Sum of entrance pupils of the Mirror Shells (corresponding to the envelope – the total area obscured by thickness of each mirror shells)

Reducing factor = Factor applied to A_{GROSS} to take into account the area lost for mechanical and assembly structures. The adopted value (0.5) has been roughly estimated on the basis of previous experiences, e.g. to design the optics of IXO mission, using the slumped glass approach.

A_{GEOM} = Effective geometrical entrance area (i.e. reducing factor x A_{GROSS}). Such value multiplied times the reflectivity to the square will give the effective area @ different energies.

Areal Efficiency = ratio A_{GEOM} over Envelope. It gives the percentage of the envelope, which is effectively used as optic. The rest is obscured by the thickness of the mirror shells and by the opto-mechanical structures. For comparison the Areal Efficiency of the ATHENA mission based on Silicon Poire Optics is 0.41 (i.e. very similar).

In Tab. 3 the mass due to the mirror shells in SiO_2 is reported for each of the six above considered optics configurations. It should be noted that, besides the mass just due to the mirror shells, it will be necessary to add the mass of the opto-mechanical structures. Based on previous experiences we suppose that we should add another 1 ton in order to account for the weight of the opto-mechanical structures.

Tab.3 Mass just due to the mirror shells (made of SiO_2) for each of the six configuration reported in Tab. 2.

ø$_{MAX}$ [m]	**MS #**	**MS thickness [mm]**	**Mass [t]**
3.125	170	2	1.08
3.11	183	1.5	0.86
3.125	200	1	0.62
3.62	187	2	1.32
3.61	201	1.5	1.05
3.61	218	1	0.75

From these preliminary considerations we can say that with SiO2 shells of 1-2 mm we can design a module pretty close to the needs of the X-ray Surveyor in terms of effective area and mass (2 tons in total).

3.2 Optical Degradation due to temperature gradients

We have preliminarily analysed the optical performance degradation related to temperature gradients (measured from manufacturing temperature) on the optics in kinematic mount conditions. In such conditions the performance degradation are simply related to the shape deformations produced by unconstrained thermal strains. Two different glass have been considered, i.e. fused silica with a CTE of 0.58×10^{-6} K^{-1} and, for comparison, D263® T eco with a CTE of 6.3×10^{-6} K^{-1}. To simplify the analysis, we have considered full (not segmented) mirror shells, subjected to reference unitary gradients (at higher temperature gradients the results can be linearly extrapolated). The optical system, shown in Fig.1, is composed by an assembly of just 3 mirror shells in Wolter 1 configuration and 10 m focal length. The mirror shells are 600mm long (300 mm + 300mm), having a radius at the parabola-hyperbola interface respectively of 500, 1000 and 1500 mm. The Finite Elements Analysis (FEA) followed by a Ray-Tracing simulation has been carried out for the three reference gradients shown in Fig. 2 (A, B, C).

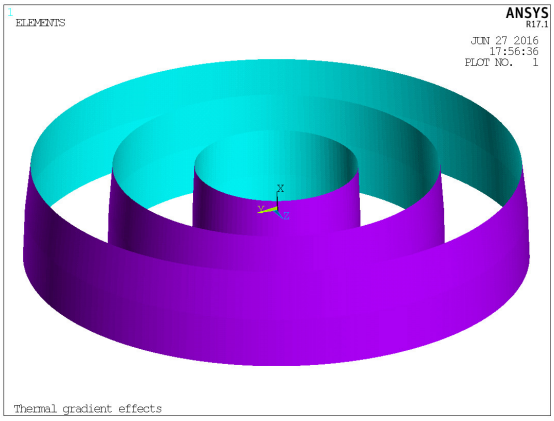

Fig. 1. The optical system considered for the preliminary study. It is an assembly of just 3 mirror shells in Wolter 1 configuration, with 10 m focal length. The radii of the shells are of 500, 1000 and 1500 mm respectively, the total length of each shell is 600 m.

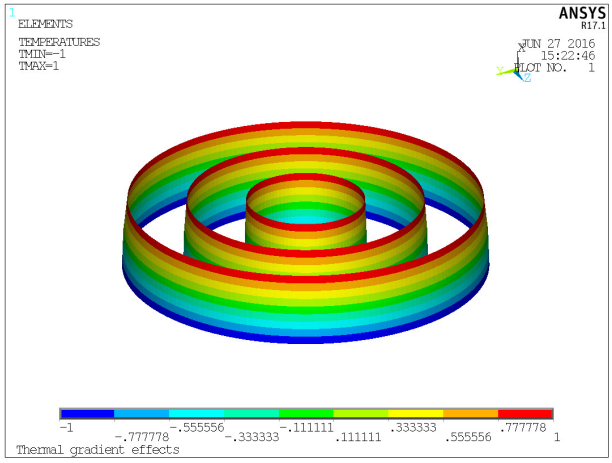

A)

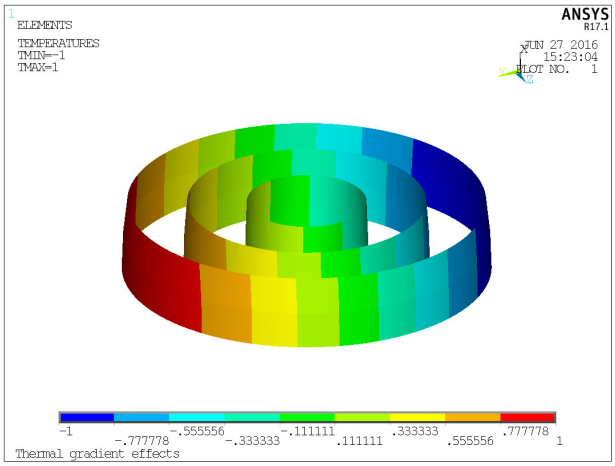

B)

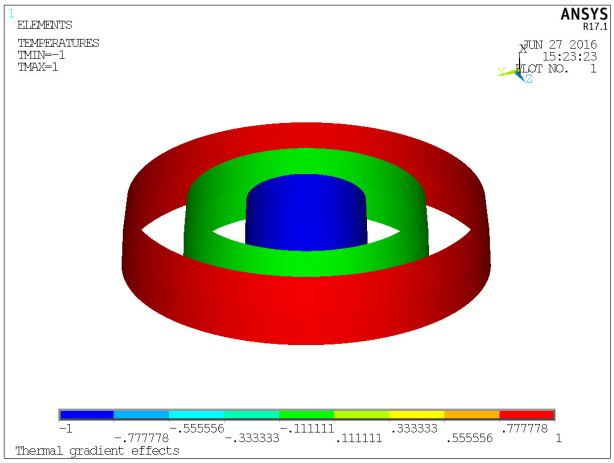

C)

Fig. 2. Thermal Gradients considered for the preliminary study ; A) T1 – Axial temperature gradients ±1K ($ø_{MAX}$ cold), B) Lateral temperature gradient (±1K) ; C) Radial temperature gradient (±1K)

The results in terms of HEW and 90%EW at the nominal and best foci are compared in Tab. 4 for the two materials considered in the analysis.

Tab. 4. HEW and 90%EW at the nominal and best foci due to the considered thermal gradients.

Temp. gradient	Material	Nominal focus		Best focus		
		HEW [arcsec]	90%EW [arcsec]	Δf [mm]	HEW [arcsec]	90%EW [arcsec]
T1 (axial)	D263® T eco	0.310	0.633	0.088	0.137	0.420
	Fused silica	0.029	0.059	-0.01	0.021	0.051
T2 (lateral)	D263® T eco	0.435	0.892	-	0.435	0.892
	Fused silica	0.041	0.084	-	0.041	0.084
T3 (radial)	D263® T eco	0.646	0.820	-0.121	0.009	0.118
	Fused silica	0.060	0.076	-0.10	0.007	0.018

The results reported in Tab.4 suggest the following remarks:

- By using fused silica it is possible to reduce the performance degradation related to temperature gradients in kinematic mounted optics by a factor 10 and more compared to the D263® T eco gladss (provided the supporting structure has an equal CTE).
- The degradation related to bulk temperature, axial and radial gradients could be largely corrected if there is the possibility to adjust the focus (for instance, in ATHENA the primary mirror is mounted on a sort of hexapod able to do that). Lateral gradient effects are not correctable by simple adjusting of the focal length.
- In segmented optics an additional degradation source could derive from the mismatch between the CTEs of the optical elements and the one of the mirror assembly structures. Such an effect can be minimized by a proper choice of the material for making the structures.

For fused silica optics, a good candidate for structural coupling materials are the Super Invar 32-5 (CTE 0.63×10^{-6} K^{-1}) (which, however, presents the drawback of a high density) and the graphite fiber-reinforced epoxy, on which CTE values very similar to fused silica have been already obtained (for instance in the HST truss).

4. THE MANUFACTURING PROCESS UNDER STUDY FOR MAKING X-RAY MIRRORS BASED ON SIO_2 SEGMENTED SUBSTRATED

In the following paragraphs we will schematically describe the main steps of the process we are setting-up with the scope to produce the grazing incidence mirrors of the X-Ray Surveyor based fused silica super-polished SiO_2 segments.

4.1 Procurement of the pre-shaped segments to be polished

The segments to be produced, before polishing, will have a single-cone or a double-cone shape; the Wolter-I profile will be imparted afterwards, after the moderation obtained with the optical polishing. In order to produce the pre-shaped segments, two methods can be used:

1. The development of pseudo-cylindrical monolithic shells and then the segments are produced by proper cuts (see Fig. 3). In this respect, one has to start from raw fused silica tubes, which are currently available on the market at affordable costs. For the present study we are working with tubes provided by Heraeus Quarzglas GmbH & Co KG. which can provides shells with diameters up to 1100 mm**.** Starting from monolithic Fused Silica glass shell, first grinding operations are performed to obtain a double cone profile at the required thickness with tolerances of few tens of microns according to a double-cone shape. After the grinding one can proceed with the operation of cutting the shell into segments by using mono-crystal diamond cutter.

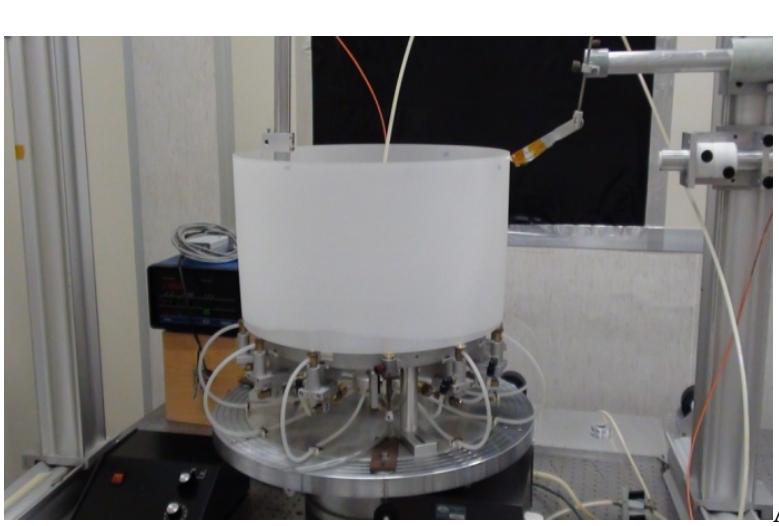
A)
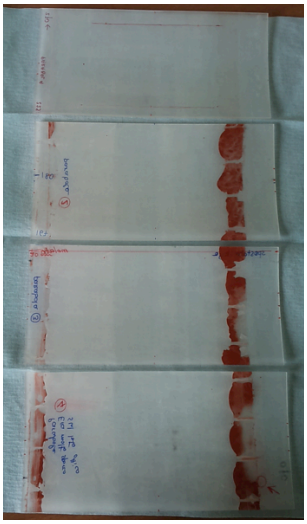
B)
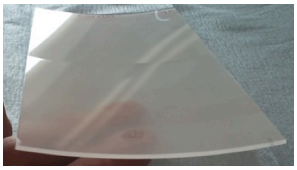
C)

Fig. 3. A) mono-lithic ground shell; B) double-cone egments produced by cutting the shell, C) double-cone single segment (in this case 100 mm x 200 mm).

2. The pre-shaping via slumping of the double cone segments. The hot-slumping process for fused silica occurs at very high temperature (> 1000 ^{o}C) and can be optimized to change from flat to the single-cone or double-cone geometries. This will reduce significantly the amount of material to be removed in raw grinding and it will allow also the manufacturing of the shells with diameters larger than 1100 mm, as required for the X-Ray Surveyor. In Fig. 4 a possible scheme for the pre-shaping via thermal slumping is presented, while in Fig. 5 an example of substrate (with pseudo-spherical shape) already produced by the Heraeus Quarzglas GmbH & Co KG company via thermal slumping in the context of a development activity aiming to set-up Near-net-Shape manufacturing process. We plan to continue the collaboration with Heraeus Quarzglas GmbH with the purpose to develop pre-shaped segments via thermal slumping specifically for the X-ray Surveyor project.

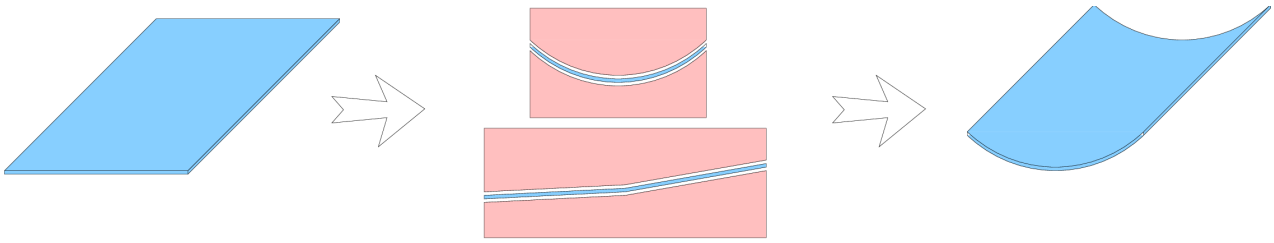

Fig. 4. Possible scheme of fused silica segments pre-shaping via thermal slumping starting from flats. For the thermal forming process each substrate is sandwiched between two molds with opposite profiles (one concave, the other convex).

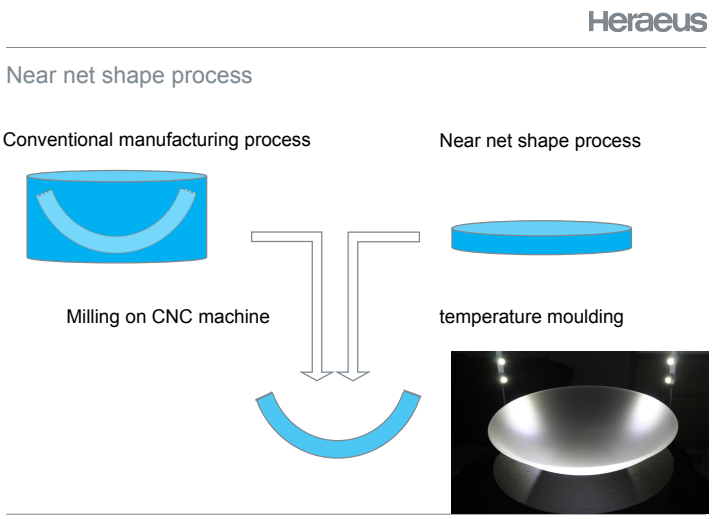

Fig. 5. Scheme of the near-net-shape process based on thermal slumping already under study at Heraeus Quarzglas GmbH & Co KG. A pseudo-spherical substrate developed in this way it is also shown (courtesy of Heraeus Quarzglas GmbH & Co KG).

4.2 Metrology and stiffening of the substrates

After the pre-shaping of the substrates, they are accurately measured and then stiffened gluing them to properly ground bulky spacer (e.g. in Aluminum). In order to speed-up the curing of the glue, one can make use of an UV-sensitive adhesive, since fused silica is transparent to the UV light. The substrate can be always detached from the spacer melting the glue in hot water (if a proper adhesive is chosen for this scope).

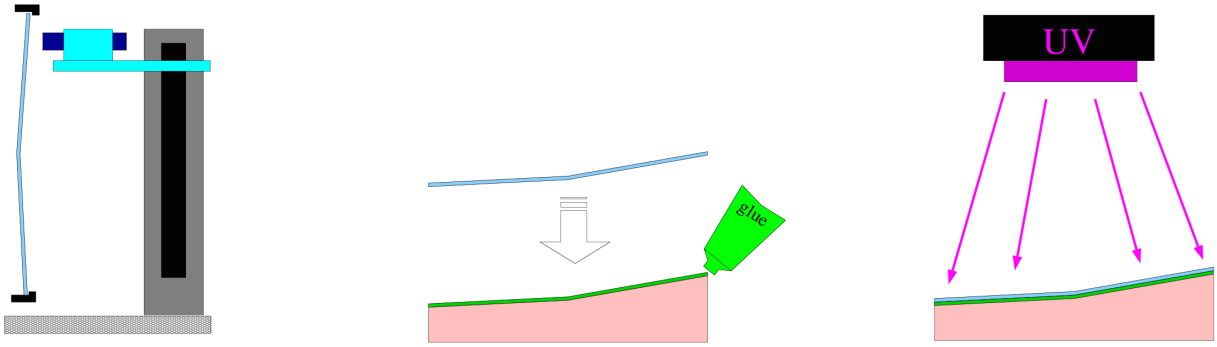

Fig. 6. Operation scheme to be carried out before starting to perform the optical polishing and figuring of the pre-shaped substrate. The substrate is measured using an astatic support and then it is glued to a bulky spacer in order to stiff it. The use of UV light speeds up the curing of the glue.

4.3 Figuring and polishing of the substrates

The figuring will be carried out via bonnet polishing, after having re-measured the profile of the substrates (Fig. 7). To this end we have equipped the premises of the Osservatorio Astronomico di Brera – INAF in Merate (Lc, Italy) with the 1200 model of the IRP (Intelligent Robotic Polisher) series machine made by Zeeko Ltd. in UK [23], aiming to support R&D and production programs also related to the development of the fused silica substrates for the X-ray Surveyor. The polishing machine is constituted of a base and bridge epoxy granite composite structures that provide good vibration damping and thermal stability. The facility has been installed into a clean room of class ISO 7 and ≈ 50 m^2 size, as shown in Fig. 7. The clean room has been built to guarantee that the manufacturing of high-value optical components

will take place in a controlled environment. The overall footprint of the facility is about $4.3m \times 4.3m \times 3m$. This includes the machine itself plus the console, a chiller unit and the slurry management unit (SMU). The largest part that can be polished is ≈ 1200 *mm* and the max load capacity is ≈500 kg. The SMU feeds the polishing process with recirculating pumped slurry maintained at constant temperature. An integrated density sensor monitors the specific gravity of the slurry.

The typical figuring process relies on a sub-aperture tool that polishes the surface and corrects its form while is going along the work-piece by following a defined path. The tool relative motion and orientation to the work-piece are ensured with great accuracy by the 7- axis computer-controlled system [24]. The linear X (Y) axis is mounted to the epoxy granite bridge (base), Z is mounted on the X assembly and perpendicular to both X and Y and to the turntable surface. The turntable accepts the work-piece and can rotate around its vertical axis C. Tool rotation axes, A, B and H, are mounted to the Z assembly. H spins the tool, which is a rubber membrane of spherical shape, named bonnet. Axes A and B intersect H at the centre of curvature of the bonnet called virtual pivot. The sphericity of the bonnet tool and the accuracy of the virtual pivot assembly guarantee the consistency of the contact spot, hence, of the removal rate, throughout the processed surface. The robotic arm is equipped with nozzles delivering the slurry of abrasive particles to the tool-work-piece contact spot.

In this method, the bonnet polishing tool is inflated by air pressure and is covered with some kind of polishing pad such as polyurethane foil. The bonnet-surface distance is preliminarily set to zero by touch, then, the bonnet is compressed against the surface by an offset of some hundreds of microns to define the spot size. Generally, the material removal rate is proportional to the relative surface speed and to the pressure applied to the part. Surface speed is mostly provided by H tool spindle. As shown in Fig. 8, the robotic arm is usually set with H axis inclined as respect to the local normal to the surface. This inclination defines the pre- cess angle, and it is intended to take the zero- velocity pole at the vertex of the bonnet out of the contact spot [25]. Since surface speed and pressure are usually set constant, the removal at any position is proportional to the time the tool is remaining there. In the form-correction process, given an error map of the surface, and a set of machine and process parameters (tool size and speed, offset, precession angle, point spacing), a dwell time map is calculated according to the removal required to correct the measured form error. Finally the machine executes the dwell time map in terms of a varying speed along the predefined tool path. By replacing the bonnet with another bigger or smaller, a larger range of spot size is made available, from few *mm* to tens of *mm*. Tools of different size target different intervals of the spatial frequency content that qualifies the error map. The minimum spot size of few *mm* roughly sets the highest spatial frequency that is correctable by bonnet polishing method. However, since the removal rate is also decreasing with the spot size, the use of small spots might be impractical, particularly when large optics are involved. The error spatial frequencies not correctable by bonnet could be effectively smoothed out by equip- ping the robotic arm with tailored pitch tools [17]). Assuming a profile error of 6 micron PtV after grinding, we have estimated a total polishing time of 40 hours to bring the surface into the prescriptions of both figure and scattering errors.

4.4 Detaching of the substrate under manufacturing from the stiffening spacer

After the polishing step, the substrate under manufacturing is detached from the stiffening spacer removing the glues. This can be easily done by the immersion into hot water at 80 ^{o}C (Fig. 9). The process lasts after 1 h.

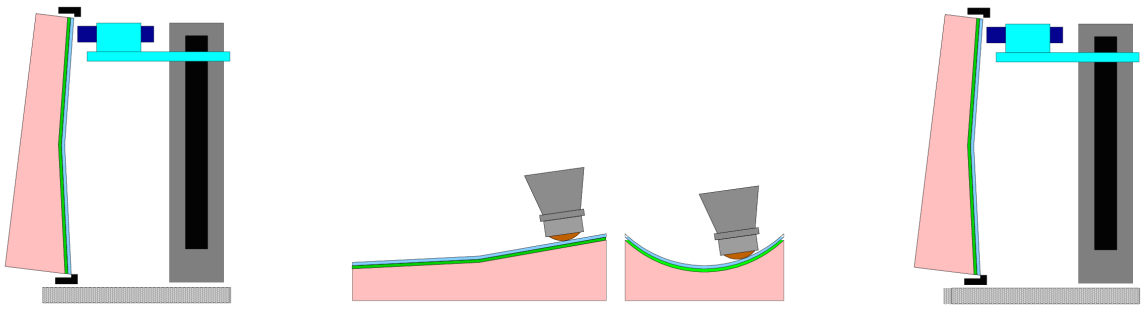

Fig. 7. Figuring step. The substrate attached to the stiffening spacer is measured and then the moderation is imparted via bonnet polishing.


A)
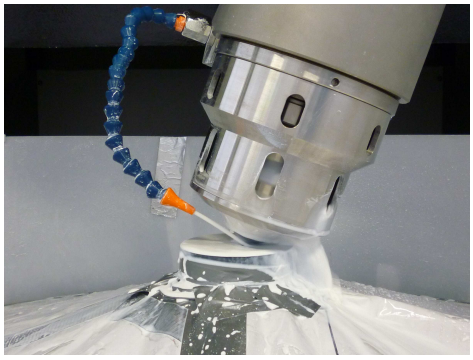
B)

Fig. 8. A) The IRP1200 series machine installed in its clean room.The console is in foreground, the SMU is partially visible on the side of the machine. B) Example of tool-part relative configuration during a polishing run.

Fig. 9. Ungluing of the substrate from the spacer in hot water.

4.5 Final correction via ion figuring

The residual low frequencies (i.e. with spatial wavelengths < 20 mm) errors on the segment surface (expected in the range of few hundreds of nm) are corrected with the Ion Beam Figuring (IBF) process. The IBF is a technique that employs an ion beam to remove in a very controlled way atomic layers of material from an optical surface in order to achieve a correct level for the shape errors (Fig. 10). INAF-OAB has built a large IBF facility (Fig.11) having a working area of 1.7 m x 1.4 m [26]. Since the mechanical frame is vertical, the movement of the ion source is in a vertical plane and also the optics to be corrected needs to be mounted vertically. The movement of the source is done in three axis, xy on the vertical area and z horizontally, to keep the distance optic-to-grids at a constant value in the case of curved optics. The maximum z sag extension is 60 mm. The ion source has two graphite grid sets having different sizes: a 50 mm collimated grid set and a 15 mm focused grid set. The first used for corrections of long spatial wavelengths, the general shape of the mirror, the second for the retouch of smaller errors, for example print through. The power of the beam can be regulated from 6 to 240 watts depending on the removal rate requested for the specific job. It should be highlighted that the ion beam figuring does not degrade the micro-roughness of the shell as far as the incoming direction of the ions in less than a few degrees [27]. Moreover, under a set of conditions, a super-smoothing effect can be achieved with final micro-roughness of 0.2 nm.

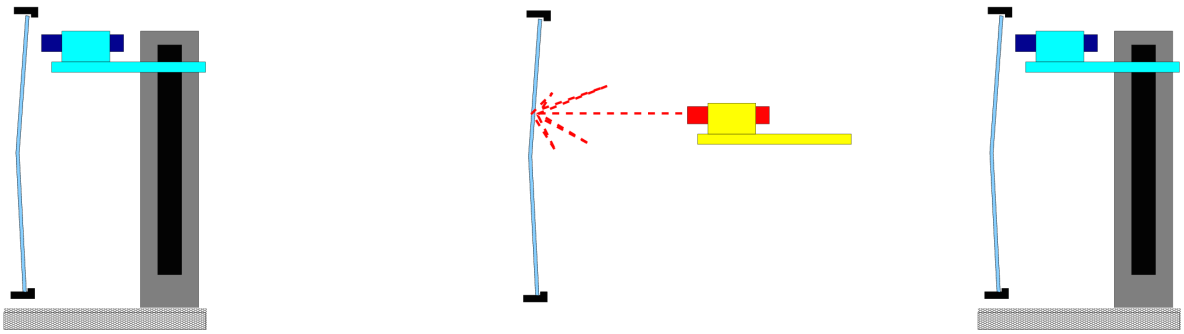

Fig. 10. Ion figuring final correction of the polished substrate, after that it has been released from the bulky spacer and a measurement of the surface error map has been done. After the ion bean figuring the substrate is measured again to verify that the desired accuracy has been achieved.

Fig. 11. The large Ion Bean Figuring facility operated at the Brera Astronomical Observatory – INAF.

Once the ion figuring of the segment has been completed and the reflecting coating deposited, then the integration on a X-Ray Mirror Unit stack using a kinematic mount can be performed.

5. PRELIMINARY RESULTS

The process described in the previous sections in under development. We plan to test the entire sequence during the next months (the procurement of raw shells to be cut has been already done). However, just before the presentation in this symposium, we have performed an useful exercise, starting from segments cut from a full monolithic (parabolic + hyperbolic profile) shell that was previously developed for the WFXT program and directly bonnet polished and also calibrated with X-rays [17]. The shell was developed with the following parameters: i) Focal length: 5500 mm, ii) Diameter at the intersection plane: 487 mm, iii) Thickness: 2 mm, iv) Total length: 200 mm, v) Material: Fused Silica. The measured HEW in X-rays of the monolithic shells was about 20 arcsec but the corresponding HEW of a segment after the cut was much higher (of the order of 45-70 arcsec), due to the release of the internal stresses. We have then performed an ion-beam correction of a of one of the segments 100 mm in width (see Fig. 3 C). In Fig. 12 it is shown the initial central profile as measured with a Long Trace Profilometer (corresponding to an HEW of 46.9 arcsec) and the expected theoretical results after the ion figuring correction of the parabolic part according to a programmed ion figuring process (corresponding to 1.1-1.2 arcsec HEW, depending on the applied filtering). The experimental results after having performed the ion-figuring process area shown in Fig. 13 (with two different filtering) as measured with two different profilometers (LTP and MPR). The corresponding HEW is 3.4 arcsec, a value that should be considered very

encouraging taking into account that the results has been achieved vey in a hurry and that the process can be greatly improved and refined.

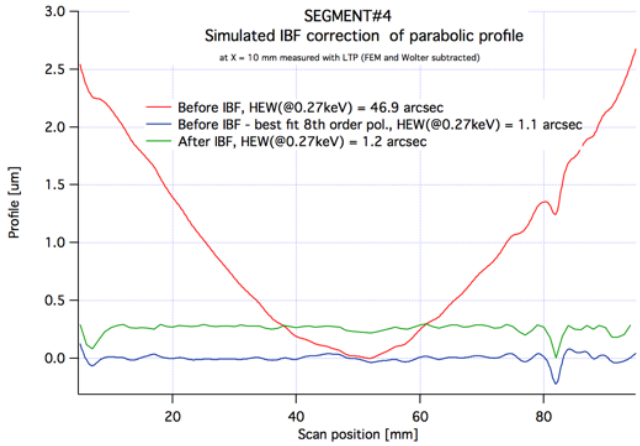

Fig. 12. Central profile of the segment cut from a previously developed WFXT shells. For comparison, we also show the expected profiles after performing a proper ion-figuring process (with two different filtering levels).

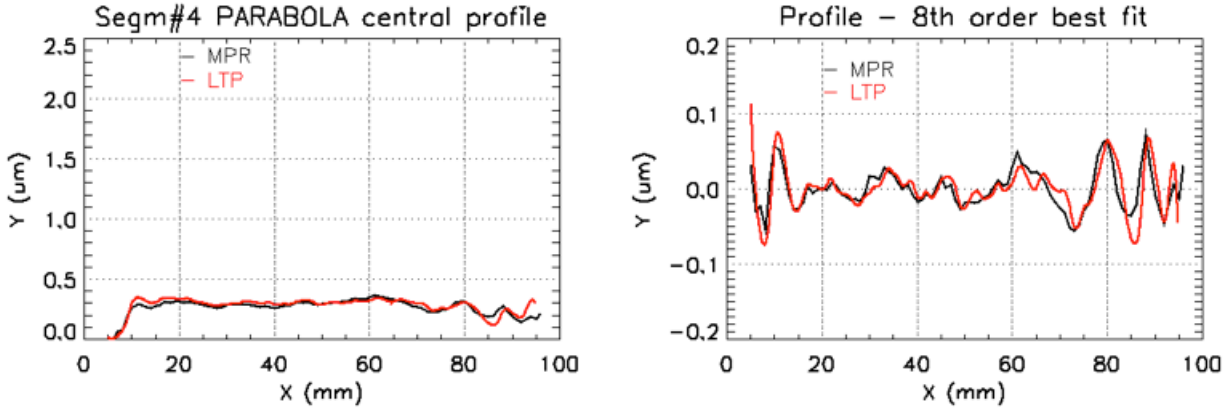

Fig. 13. Real Central profile of the segment cut from a previously developed WFXT shells after having performed the ion-figuring treatment. The profiles have been measured with two different profilometers (LTP and MPR). The corresponding HEW is 3.4 arcsec.

6. CONCLUSIONS

In this paper we have discussed a new process aiming at the realization of an X-ray telescope with an angular resolution similar to Chandra but with much larger effective area and field of view, like the X-Ray Surveyor project. A new process based on direct-polishing and ion-figuring correction of Fused Silica slabs is being set-up. We aim to demonstrate that the X-ray Surveyor angular resolution requirement can be achieved following this production approach for making the X-ray mirrors. Preliminary considerations on the use of Fused Silica slabs for the mirrors of the X-ray Surveyor telescope give very promising results in terms of opto-mechanical and thermal performances. Samples are under development. Preliminary results obtained with an initial sample are very encouraging. We plan to verify the entire procedure during next months and to organize X-ray calibrations soon.

ACKNOWLEDGMENTS

This research is supported by the Italian space Agency (ASI). We warmly acknowledge Heraeus Quarzglas GmbH & Co, LT Ultra Precision Technology GmbH KG. and MEDIA LARIO for the cooperation in the development of the project presented in this paper.

REFERENCES

[1] Weisskopf, M.C., et al., “Chandra X-ray Observatory (CXO): overview”, Proc. SPIE Vol. 4012, p. 2-16 (2000)
[2] Weisskopf, M.C.; O'dell, S. L.; van Speybroeck, L. P., ”Advanced X-Ray Astrophysics Facility (AXAF)”, Proc. SPIE Vol. 2805, p. 2-7 (1996)
[3] van Speybroeck, L. P., et al., “Performanpectation versus reality”, Proc. SPIE Vol. 3113, p. 89-104 (1997).
[4] Bavdaz, M., et al., “The evolving universe spectroscopy mission (XEUS)”, Proc. SPIE Vol. 4012, p. 306-315, X-Ray Optic (2000)
[5] Nandra, K., et al., “The Hot and Energetic Universe: A White Paper presenting the science theme motivating the Athena+ mission”, White Papers for the definition of the L2 and L3 missions in the ESA Science program. More information: http://www.the-athena-x-ray-observatory.eu/, 2013arXiv1306.2307N
[6] Willingale, R., Pareschi, G., Christensen, F., den Herder, J.-W., Ferreira, D., Jakobsen, A., Ackermann, M., Collon, M., Bavdaz, M., “Science requirements and optimization of the silicon pore optics design for the Athena mirror”, Proceedings of the SPIE, Volume 9144, id. 91442E 9 pp. (2014)
[7] A. Vikhlinin, et al., “SMART-X, “Square Meter, Arcsecond Resolution X-ray Telescope”, et al., Proc. "X-ray Astronomy: the next 50 years", Mem SAIt, in press (2013)
[8] Gaskin, J. A., et al, “The X-ray Surveyor Mission: A Concept Study”, Proc. SPIE Vol. 9601-18 (2015)
[9] Zhang, W. W., et al., “High resolution and high throughput x-ray optics for future astronomical missions”,Proc. SPIE Vol. 8861, in press (2013, present volume)
[10] Schattenburg, M. L., Chalifoux, B., DeTienne, M. D., Heilmann, R. K., Zuo, H., “Progress report on air bearing slumping of thin glass mirrors for x-ray telescopes”, Proceedings of the SPIE, Volume 9603, id. 96030R 8 pp. (2015).
[11] Salmaso, B., et al., “Slumped glass optics development with pressure assistance”, Proceedings of the SPIE, Volume [9905-71], in press (2016)
[12] Cotroneo, V., et al., “Thermal forming of glass substrates for X-ray Surveyor optics”, Proceedings of the SPIE, Volume [9905-215], in press (2016)
[13] Allured, R., et al., “Improved control and characterization of adjustable x-ray optics”, Proc. SPIE, Volume 9603, id. 96031M 10 pp. (2015).
[14] Yao, Y., Wang, X., Cao, J., Ulmer, M., “Stress manipulated coating for fabricating lightweight X-ray telescope mirrors”, Optics Express, vol. 23, issue 22, p. 28605 (2015).
[15] Chalifoux, B., Wright, G., Heilmann, R. K., Schattenburg, M. L., “Ion implantation for figure correction of thin X-ray telescope mirror substrates”, Proceedings of the SPIE, Volume 9603, id. 96031K 15 pp. (2015).
[16] Zhang, W.W., et al., “High-resolution lightweight x-ray optics”, Proceedings of the SPIE, Volume [9905-60], in press (2016)
[17] Citterio, O., et al., “Progress on precise grinding and polishing of thin glass monolithic shell (towards WFXT)”, Proceedings of the SPIE, Volume 8147, article id. 814714, 11 pp. (2011)
[18] Proserpio, L., et al., ”Design and development of thin quartz glass WFXT polynomial mirror shells by direct polishing”, Proceedings of the SPIE, Volume 7732, article id. 77320D, 14 pp. (2010).
[19] Gubarev, M., et al, “Development of the a direct fabrication technique for full-shell x-ray optic”, Proceedings of the SPIE, Volume [9905-63], in press (2016)
[20] Atkins, C., et al, “Differential deposition correction of segmented glass x-ray optics”, Proceedings of the SPIE, Volume 9603, id. 96031G 14 pp. (2015).
[21] Ghigo, M., et al., “Ion figuring of large prototype mirror segments for the E-ELT”, Proceedings of the SPIE, Volume 9151, id. 91510Q 12 pp. (2014).
[22] van Speybroeck, L. P., “Design, fabrication and expected performance of the HEAO-B X ray telescope”, Proceedings of the Seminar, Reston, Va., (A78-40248 17-35) Bellingham, Wash., Society of Photo-Optical Instrumentation Engineers, 1977, p. 136-143 (1977)
[23] G. Vecchi, S. Basso, M. Civitani, M. Ghigo, G. Pareschi, M. Riva and F. M. Zerbi
“A bonnet and fluid jet polishing facility for optics fabrication related to the E-ELT”, *Mem. SAIt,,* Vol.86 n.3, 408 (2015)
[24] D. D. Walker, et al., "Precessions process for efficient production of aspheric optics for large telescopes and their instrumentation", Proc. SPIE, 4451, 267 (2002)

[25] Walker, D. D., et al. 2006, Proc. of SPIE, 6273, 627309
[26] Ghigo, M., Cornelli, S., Canestrari, R. , Garegnani, D. , "Development of a large ion beam figuring facility for correction of optics up to 1.7 m diameter", Proc. SPIE 7426, 742611 (2009)
[27] Wenin Liao, Yifan Dai, Xuhui Xie, and Lin Zhou, "Morphology evolution of fused silica surface during ion beam figuring of high-slope optical components", Appl. Opt. 52, 3719-3725 (2013)